

# Theory of ion transport with fast acid-base equilibrations in bioelectrochemical systems

J. E. Dykstra,<sup>1,2</sup> P. M. Biesheuvel,<sup>2,3</sup> H. Bruning,<sup>1</sup> and A. Ter Heijne<sup>1,\*</sup>

<sup>1</sup>*Sub-department of Environmental Technology, Wageningen University, Bornse Weilanden 9, 6708 WG Wageningen, The Netherlands*

<sup>2</sup>*Wetsus, centre of excellence for sustainable water technology, Oostergoweg 7, 8911 MA Leeuwarden, The Netherlands*

<sup>3</sup>*Laboratory of Physical Chemistry and Colloid Science, Wageningen University, Dreijenplein 6, 6703 HB Wageningen, The Netherlands*

(Received 2 February 2014; published 2 July 2014)

Bioelectrochemical systems recover valuable components and energy in the form of hydrogen or electricity from aqueous organic streams. We derive a one-dimensional steady-state model for ion transport in a bioelectrochemical system, with the ions subject to diffusional and electrical forces. Since most of the ionic species can undergo acid-base reactions, ion transport is combined in our model with infinitely fast ion acid-base equilibrations. The model describes the current-induced ammonia evaporation and recovery at the cathode side of a bioelectrochemical system that runs on an organic stream containing ammonium ions. We identify that the rate of ammonia evaporation depends not only on the current but also on the flow rate of gas in the cathode chamber, the diffusion of ammonia from the cathode back into the anode chamber, through the ion exchange membrane placed in between, and the membrane charge density.

DOI: [10.1103/PhysRevE.90.013302](https://doi.org/10.1103/PhysRevE.90.013302)

PACS number(s): 02.70.-c, 82.39.Wj, 82.47.Wx, 82.60.Hc

## I. INTRODUCTION

Bioelectrochemical systems (BESs) are electrochemical cells that use micro-organisms as the catalyst of reactions at one of the electrodes. A BES can recover electrical energy from aqueous organic waste streams (the microbial fuel cell, henceforth MFC) [1–6], or produce chemicals, such as H<sub>2</sub>, from the same streams, using an electrical energy input (the microbial electrolysis cell, henceforth MEC) [7–11]. In a conventional BES, a biofilm develops at the anode where micro-organisms oxidize the substrate, which is organic matter. Electrons are released to the anode and are transported via an electrical circuit to the cathode, where they are used for the reduction of oxygen gas to OH<sup>−</sup> ions (MFC) or for the reduction of protons to hydrogen gas (MEC). In an MFC, the reaction is thermodynamically favorable, and therefore electrical energy can be recovered. On the other hand, in an MEC, an electrical energy input is required to drive the reaction, and the energy from the aqueous organic streams together with the electrical energy input is recovered as chemical energy in the form of hydrogen gas (H<sub>2</sub>). Both for an MFC and an MEC system, for every electron transported from the anode to the cathode, simultaneously an ion migrates from the anode to the cathode compartment, or in the other direction, to keep the solutions electroneutral [5]. The anode and cathode compartments are typically separated by an ion-exchange membrane, which allows preferential passage of either ions with a positive or ions with a negative charge. For instance, a cation-exchange membrane mainly allows passage for the cations to move from the anode to the cathode compartment.

An organic waste stream of particular interest for BES technology is urine, because urine has a high concentration of organic matter, typically 10 g L<sup>−1</sup> COD (chemical oxygen demand), and it contains significant amounts of the nutrients nitrogen (10 g L<sup>−1</sup>) and phosphorus (1 g L<sup>−1</sup>), concentrations that are higher than in other wastewater streams [12,13]. Kuntke *et al.* [14,15] discuss the possibility of combining

the production of electrical energy with the recovery of ammonia gas in a U-MFC (with U for urine), or to combine ammonia recovery with the production of hydrogen gas, in a U-MEC. In a U-MEC, organic matter is oxidized by micro-organisms on the anode. Electrons are transported from the anode through the electrical circuit to the cathode, where protons are reduced to hydrogen gas. The cathode is typically made of a porous carbon film electrode, and is wetted, i.e., filled with electrolyte, and directly faces the ion-exchange membrane on one side and the gas diffusion chamber on the other side; see Fig. 1. Because of the high ammonium ion (NH<sub>4</sub><sup>+</sup>) concentration in urine, ammonium is considered to be the main carrier of protons from the anode chamber to the cathode [16]. Due to the high pH in the cathode, the ammonium ion is converted here to ammonia (NH<sub>3</sub>), which evaporates into the gas diffusion cathode chamber and in this way is recovered. This approach combines the advantages of removing ammonium from wastewater, which is normally an energy-intensive process, with the production of ammonia, which has value as a component in the production of fertilizer [17]. An overview of this process is shown in Fig. 1. In the present work, we will quantitatively analyze transport of all ions through the ion-exchange membrane and the simultaneous formation of H<sub>2</sub> and NH<sub>3</sub> in gaseous form.

In Refs. [14,18] it was reported that although ammonia was successfully recovered from the cathode, the actual ammonia removal was less than expected. Therefore, to analyze this MEC technology in more detail, including current-induced ammonia evaporation, we developed a theoretical model that includes the transport of ions from the anode chamber toward the cathode, as well as their transport in the reverse direction. Because most ions in the system are amphoteric, that is, they can react as acid as well as a base, this model needs to incorporate the ion acid-base equilibrium reactions that take place in solution and in the membrane. One example of such a reaction is the one involving ammonia (NH<sub>3</sub>), a proton, and the ammonium ion (NH<sub>4</sub><sup>+</sup>).

Transport models with amphoteric ions are frequently used, but they can have very different underlying assumptions. These models, including amphoteric ions, are used for instance to

\*Corresponding author: [annemiek.terheijne@wur.nl](mailto:annemiek.terheijne@wur.nl)

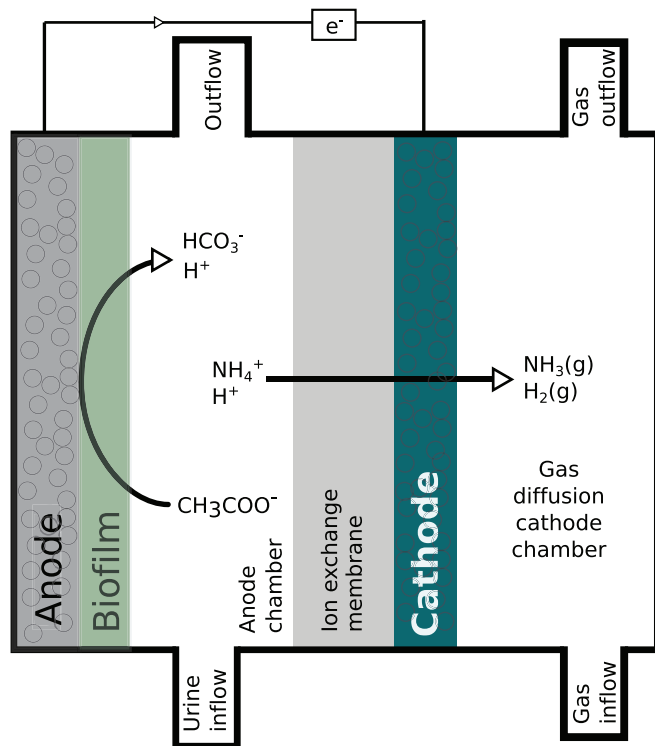


FIG. 1. (Color online) Schematic view of a bioelectrochemical system that recovers both chemical energy (in the form of  $H_2$ ) and ammonia from urine.

model transport across biofilms [19], across ion-exchange membranes [20], and around plant leaves submerged in water [21]. We will discuss four different types of models that incorporate amphoteric ions, after which we will introduce our approach to model current-induced ammonia evaporation in an MEC.

(i) Often, all ion types (e.g.,  $NH_3$ ,  $NH_4^+$ ) are lumped together and described as one uncharged species, such as  $NH_3$ . In these models, Fick's law is used to model ion transport only subject to diffusional forces. These models [22–24] do not incorporate acid-base equilibria, and therefore they do not describe, for instance, the effect of pH on adsorption and transport.

(ii) More detailed models [19,20,25–28] do include the acid-base reactions of the amphoteric ions. All ion types ( $NH_3$ ,  $NH_4^+$ ) are separately considered, rather than lumping them together. In this approach, Fick's law is still used, considering only diffusional transport, neglecting the migration of ions due to the electrical field. However, such an electrical field always develops, also in the absence of an applied current, except for zero current and the unlikely situation that all ions have the same diffusion coefficient.

(iii) In more advanced ionic transport models, the effect of the electrical field on the diffusion of ions is included, as well as the acid-base reactions [29,30]. To describe the acid-base reactions, a rate equation such as  $r = k_f[HCO_3^-] - k_b[CO_3^{2-}][H^+]$  is used, where  $k_f$  and  $k_b$  are the forward and backward rate constants. One problem in this approach is that because the acid-base reactions are fast,  $k_f$  and  $k_b$  have very high values. Since diffusion and migration of ionic species is

much slower, a set of numerically stiff equations results, which are difficult to solve.

(iv) To make this calculation numerically much simpler, it is very useful to assume that in the membrane and in solution all of the acid-base reactions are infinitely fast. The resulting acid-base equilibria can be directly incorporated in the ionic mass balances. As a result, the model does not make use of the rate constants,  $k_f$  and  $k_b$ , but only uses the pK value of the respective equilibrium [21,31–36]. Thus, in this approach, a kinetic equation with rate constants does not need to be considered.

We will demonstrate how this category (iv) approach can be used to set up a simple and robust one-dimensional steady-state model for the transport and recovery of valuable compounds, in this case ammonia, in bioelectrochemical systems. Therefore, we combine in our model the following two elements: (i) the acid-base equilibria directly implemented in the individual ion mass balance equations for transport through a charged ion-exchange membrane; and (ii) the direct coupling of the ionic transport to the electrical current, to the hydrogen gas production, and to the evaporation of ammonia in an electrolyte-filled porous electrode in contact with a gas phase.

To our knowledge, this combination of modeling elements has not yet been described in the literature. The one-dimensional steady-state model will be used to describe ion transport from the anode to the cathode through different types of membranes in a U-MEC. To show the practical relevance of such a modeling framework, we will identify the influence on the evaporation of ammonia and the production of hydrogen of several key engineering parameters, such as the flow rate of inert gas along the cathode and the pressure in the cathode chamber.

## II. THEORY

In this section, we present a steady-state BES model that links the reactions on the anode and on the cathode to the electrical current. This electrical current drives ion transport through the membrane located near the cathode. The cathode is a porous carbon film electrode, which is filled with electrolyte; see Fig. 2. The cathode faces the membrane on one side and faces the gas diffusion chamber on the other side, with direct contact between the gas and the liquid. In the cathode, we assume the ion transport to be fast compared to that in the membrane. We focus on ion transport in the membrane and the evaporation of ammonia from the cathode, and we will use the current density, not the cell voltage, as an independent variable for our simulation. An overview of the ion types incorporated in the model is presented in Fig. 2.

To simplify matters, in this paper we consider that the inlet stream, urine, contains the following mixture of dissolved ions: salt ions that do not react ( $Na^+$  and  $Cl^-$ ); organic matter, represented by acetic acid (HAc) and the acetate ion ( $Ac^-$ ); next the carbonic acid ( $H_2CO_3$ ), bicarbonate ( $HCO_3^-$ ), and carbonate ions ( $CO_3^{2-}$ ); and finally the ammonium ion and dissolved ammonia; see Table I. As explained before, the concentrations of ions are coupled via their acid-base equilibrium reactions, such as those of acetic acid and acetate. This has the consequence that in the numerical model, the concentration of only one of these amphoteric ions (henceforth

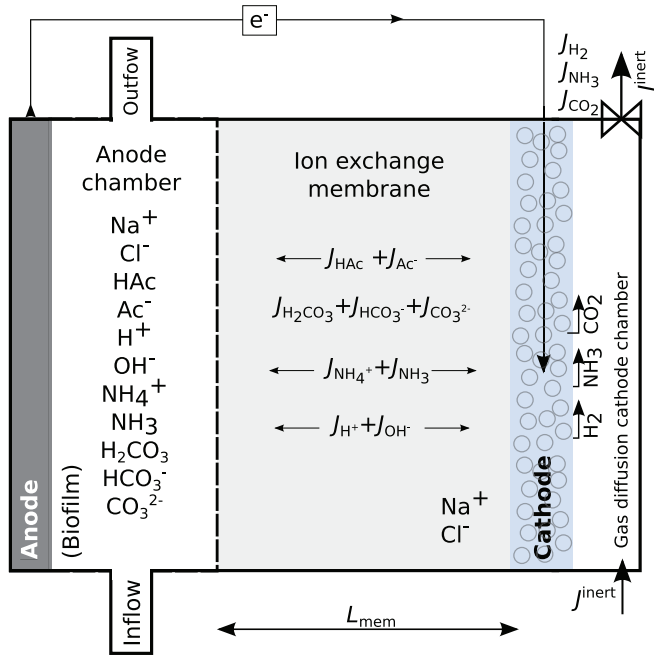


FIG. 2. (Color online) Schematic view of ionic fluxes and electrochemical reactions incorporated in the BES model. The ionic current due to the combined transport of all ionic species from the anode chamber to the cathode is directly connected to the electrical current. Sizes are not to scale: in reality, the anode chamber is several cm wide while the membrane thickness is only a few hundred  $\mu\text{m}$ .

called the “key ion”) is considered in the mass balances, and the concentration of the other ion(s) from this group can be calculated *a posteriori* from the acid-base equilibria; see the section on equilibrium constants in Table I. This holds for acetate and as well for the group comprising ammonium and ammonia (where we choose ammonium as the key ion), and for the group consisting of carbonic acid, bicarbonate, and carbonate ions (where we choose bicarbonate as the key ion).

### A. Transport across the ion-exchange membrane

In the BES for current-induced ammonia evaporation, the ion-exchange membrane (IEM) is an essential element. In the present work, we assume that the entire resistance for ion transport from the anode chamber to the cathode is located in this membrane. The IEM is characterized by its membrane charge density due to groups of a fixed charge in the membrane. Effectively, this membrane charge leads to selective transport, where counterion transport through the IEM is enhanced and co-ion transport is hindered. Counterions are ions with a charge sign opposite to that of the membrane fixed charge groups, while co-ions have the same charge sign as the membrane. We can distinguish between an anion exchange membrane, where anions are the counterions, and a cation exchange membrane, where cations are the counterions. The transport of uncharged species is not directly influenced by the charge of the membrane, and they are transported through the membrane by diffusional forces only. So, the background charge of the membrane does not enhance the transport of the uncharged species, nor does it hinder these species. Note that our model

does not consider ionic transport in one direction only, but instead all fluxes and the direction thereof are self-consistently calculated by the model. Thus, the possible migration and diffusion of ions from the cathode back to the anode chamber is naturally included.

Ionic diffusion and electromigration through the membrane are described using the Nernst-Planck equation,

$$J_i = -D_{e,i} \left( \frac{\partial c_i}{\partial x} + z_i c_i \frac{\partial \phi}{\partial x} \right), \quad (1)$$

where the subscript  $i$  refers to the ionic species  $i$ ,  $J$  is the ionic flux ( $\text{mol m}^{-2} \text{s}^{-1}$ ),  $D_e$  is the effective diffusion coefficient ( $\text{m}^2 \text{s}^{-1}$ ),  $c$  is the ion concentration per volume aqueous phase in the membrane ( $\text{mol/m}^3$ ),  $x$  is the coordinate running from  $x = 0$  to  $x = L_{\text{mem}}$ ,  $z$  is the ionic charge number (e.g., +1 for  $\text{Na}^+$ ), and  $\frac{\partial \phi}{\partial x}$  is the electrical potential gradient. Here,  $\phi$  is a dimensionless electrical potential, which can be multiplied by the thermal voltage,  $V_T = \frac{RT}{F}$ , with  $R$  the gas constant ( $\frac{\text{J}}{\text{mol K}}$ ),  $T$  the temperature (K), and  $F$  Faraday’s constant (C/mol), to obtain the voltage with dimension  $V$ . The effective diffusion coefficient is a certain fraction of the value in a free (dilute) solution,  $D_{\text{aq},i}$ . We choose the same fraction,  $d_f$ , for all ions, thus  $D_{e,i} = D_{\text{aq},i} d_f$ .

Except for the Donnan boundary layers located at each membrane outer surface, the electroneutrality condition holds at each position in the membrane,

$$\sum_i z_i c_i + \omega X = 0, \quad (2)$$

where  $\omega$  is the sign of the membrane charge (+1 for AEM and 1 for CEM) and  $X$  is the membrane charge expressed in moles per unit aqueous phase in the membrane [37]. The summation runs over all the ions,  $i$ , present in the system.

The mass balance equation of every species is described by the partial differential equation

$$\frac{\partial c_i}{\partial t} = -\frac{\partial J_i}{\partial x} + \Gamma_i \quad (3)$$

with  $t$  time (s) and  $\Gamma_i$  the formation rate of species  $i$  ( $\text{mol m}^3 \text{s}^{-1}$ ). In this work, we only compute the steady-state solution, and therefore the accumulation term,  $\frac{\partial c_i}{\partial t}$ , is set to 0.

How do we incorporate the production and/or consumption of ions by the acid-base equilibria in the system? Let us illustrate our approach using the ammonium-ammonia equilibrium as an example. Since at each position the production of ammonia,  $\Gamma_{\text{NH}_3}$ , equals the consumption of ammonium ions,  $\Gamma_{\text{NH}_4^+}$ , the following equality must hold, namely that  $\Gamma_{\text{NH}_3} = -\Gamma_{\text{NH}_4^+}$ . Note that this is also true in a dynamic situation when  $\frac{\partial c_i}{\partial t}$  is not zero. What is assumed, however, is that these ions do not participate in any other (equilibrium) reaction, such as the formation of the carbamate ion by the reaction  $\text{HCO}_3^- + \text{NH}_3 \leftrightarrow \text{NH}_2\text{CO}_2^- + \text{H}_2\text{O}$  [38]. In the case we consider, we sum Eq. (3) over the different ionic species in a group of amphoteric ions, and the production and consumption terms cancel out. Subsequently, the resulting equation, which is a function of the concentrations of  $\text{NH}_3$  and  $\text{NH}_4^+$  and a function of the potential  $\phi$ , is discretized at a predefined number of nodes, employing the finite-difference method. The resulting set of algebraic equations can be solved

TABLE I. Parameters used in the BES model (Refs. [14,40];  $T = 298$  K).

$L_{\text{mem}}$	Thickness of the membrane ( $\mu\text{m}$ )		100
$J_G^{\text{inert}}$	Inert-gas flow rate through the cathode gas chamber (mol/s) divided by the surface area of the membrane ( $\text{m}^2$ ), which is equal to the electrode area		0.01
$p_{\text{tot}}$	Pressure in the cathode gas chamber (bar)		1
		Concentrations in anode chamber (mM)	Diffusion coefficients in free solution ( $\cdot 10^{-9} \text{ m}^2/\text{s}$ )
HAc	Acetic acid	0.00528	1.21
$\text{Ac}^-$	Acetate	65.0	1.10
$\text{H}_2\text{CO}_3$	Carbonic acid	0.0153	1.92
$\text{HCO}_3^-$	Bicarbonate	4.82	1.18
$\text{CO}_3^{2-}$	Carbonate	0.16	0.98
$\text{NH}_4^+$	Ammonium	161	1.94
$\text{NH}_3$	Ammonia	64.1	2.10
$\text{Na}^+$	Sodium	80.4	1.33
$\text{Cl}^-$	Chloride	171	2.02
$\text{H}^+$	Proton, hydronium ion		9.13
$\text{OH}^-$	Hydroxyl ion		5.16
pH		8.85	
Equilibrium constants			
$pK_{\text{a,AC}}$	$\text{CH}_3\text{COOH} \longleftrightarrow \text{CH}_3\text{COO}^- + \text{H}^+$	$K_{\text{a,AC}} = \frac{[\text{CH}_3\text{COO}^-][\text{H}^+]}{[\text{CH}_3\text{COOH}]}$	4.76
$pK_{\text{a,CA1}}$	$\text{H}_2\text{CO}_3 \longleftrightarrow \text{HCO}_3^- + \text{H}^+$	$K_{\text{a,CA1}} = \frac{[\text{HCO}_3^-][\text{H}^+]}{[\text{H}_2\text{CO}_3]}$	6.35
$pK_{\text{a,CA2}}$	$\text{HCO}_3^- \longleftrightarrow \text{CO}_3^{2-} + \text{H}^+$	$K_{\text{a,CA2}} = \frac{[\text{CO}_3^{2-}][\text{H}^+]}{[\text{HCO}_3^-]}$	10.33
$pK_{\text{a,NH}}$	$\text{NH}_4^+ \longleftrightarrow \text{NH}_3 + \text{H}^+$	$K_{\text{a,NH}} = \frac{[\text{NH}_3][\text{H}^+]}{[\text{NH}_4^+]}$	9.25
$pK_w$	$\text{H}_2\text{O} \longleftrightarrow \text{OH}^- + \text{H}^+$	$K_w = [\text{H}^+][\text{OH}^-]$	14.00
Note that $K_a$ (with unit mM) relates to the $pK_a$ values using $^{10}\log(K_a) = 3 - pK_a$ , because the concentrations in our model are calculated in $\text{mol}/\text{m}^3$ (mM). $K_w$ (with unit $\text{mM}^2$ ) relates to $pK_w$ using $^{10}\log(K_w) = 6 - pK_w$ . Square brackets [...] denote concentration in mM.			
Henry coefficients (mM/bar)			
$K_{\text{H,CO}_2}$	carbon dioxide		33.46
$K_{\text{H,NH}_3}$	ammonia		56250
$d_f$	Effective diffusion coefficients in membrane in relation to values in free (dilute) solution (-)		0.1

together with the equilibrium relations,

$$K_{\text{a,NH}} = \frac{[\text{NH}_3][\text{H}^+]}{[\text{NH}_4^+]}, \quad (4)$$

which are listed in Table I. (Note that in this work we use both the notation [...] and the symbol  $c$  to describe concentrations.) However, to reduce the number of equations significantly, we can implement Eq. (4) in the discretized transport equations such that only the concentration of the key ion (in this example the ammonium ion) and the concentration of the proton remain, and the other ions are no longer part of the numerical scheme. Thus, the procedure is as follows. By substituting the equilibrium relations, such as Eq. (4), into Eq. (3), one can eliminate either the variable  $[\text{NH}_3]$  or  $[\text{NH}_4^+]$  and obtain a mass balance equation only dependent on three variables, namely the concentration of the key ion, the concentration of protons, and the local potential  $\phi$ .

The same approach of replacing the concentrations of the monkey ions by the concentration of the key ion and of the proton is also employed for the acetate and acetic acid ions, with acetic acid as the key ion, and for the carbonic acid, bicarbonate, and carbonate ions, with bicarbonate as the key ion. We furthermore consider the electroneutrality condition, Eq. (2), and the charge balance, which describes that at each position the divergence of the ionic current is 0,

$$\frac{\partial}{\partial x} \sum_i z_i J_i = 0. \quad (5)$$

In the charge balance, Eq. (5), we substitute Eq. (1). The resulting equation is discretized, after which we substitute the equilibrium conditions, as listed in Table I, to eliminate the variables  $[\text{CO}_3^{2-}]$  and  $[\text{OH}^-]$  ( $\text{NH}_3$ ,  $\text{H}_2\text{CO}_3$ , and HAc are not in this balance because  $z = 0$  for these species). This set of equations suffices to describe ion transport. Note that we do not set up a balance for the proton or hydroxyl ion.

Because of steady state and the absence of reactions involving the nonamphoteric ions  $\text{Na}^+$  and  $\text{Cl}^-$ , there is no net flux of these two ions across the membrane. Therefore, the concentration of these ions is only dependent on the local potential and is, according to the Boltzmann distribution, given by

$$c_{A,i} = c_{B,i} \exp(-z_i \Delta\phi_{AB}) \quad (6)$$

with  $c_{A,i}$  the concentration on location A,  $c_{B,i}$  the concentration on location B, and  $\Delta\phi_{AB}$  the potential difference between locations A and B. Note that Eq. (6) follows from Eq. (1) after setting the flux,  $J$ , to zero.

On the interface of the anode chamber with the membrane, the concentration of the ions on the membrane side of this interface ( $c_{\text{mem}}$ ) relates directly to the concentration in the anode chamber ( $c_{\text{an}}$ ) according to the Donnan equilibrium [37],

$$c_{\text{mem},i} = c_{\text{an},i} \exp(-z_i \Delta\phi_D), \quad (7)$$

where  $\Delta\phi_D$  is the Donnan potential drop, i.e., the potential just inside the membrane, minus that in the anode chamber. We assume the water flow rate through the anode chamber to be high compared to the membrane flux, so we assume that the concentrations in the anode chamber are equal to the inflow concentrations, as given in Table I.

### B. Reactions on the cathode

In the cathode, we link the various fluxes (production of  $\text{H}_2$ , evaporation of  $\text{NH}_3$ , and  $\text{CO}_2$ ) to one another, and to the electrical current. Assuming that hydrogen gas formation is the only occurring Faradaic reaction, and assuming the absorption of  $\text{H}_2$  in the liquid phase to be zero, we can relate the hydrogen gas production flux  $J_{\text{H}_2}^{\text{evap}}$  (flow rate per unit membrane area, in  $\text{mol m}^{-2} \text{s}^{-1}$ ) to the current,  $I$  ( $\text{A m}^{-2}$ ), by

$$I = 2F J_{\text{H}_2}^{\text{evap}}, \quad (8)$$

where the factor “2” is due to the fact that always two electrons are required to form one hydrogen gas molecule.

The sum of the ionic fluxes ( $\text{mol m}^{-2} \text{s}^{-1}$ ) of  $\text{NH}_3$ ,  $J_{\text{NH}_3}^{\text{C}}$ , and  $\text{NH}_4^+$ ,  $J_{\text{NH}_4^+}^{\text{C}}$ , through the membrane, evaluated at the edge with the cathode (denoted by superscript “C” from this point onward), equals the evaporation flux of  $\text{NH}_3$ ,  $J_{\text{NH}_3}^{\text{evap}}$  ( $\text{mol m}^{-2} \text{s}^{-1}$ ),

$$J_{\text{NH}_3}^{\text{evap}} = J_{\text{NH}_4^+}^{\text{C}} + J_{\text{NH}_3}^{\text{C}}. \quad (9)$$

Note that, interestingly, it is the sum of the fluxes of ammonia and ammonium in the membrane, which together are equal to the ammonia gaseous evaporative flux. This follows from the fact of zero accumulation of N atoms at the gas-liquid surface, in combination with the assumed infinitely fast equilibration of  $\text{NH}_4^+$  with  $\text{NH}_3$  in the aqueous phase.

The evaporation flux of gaseous  $\text{CO}_2$ ,  $J_{\text{CO}_2}^{\text{evap}}$ , relates to the membrane fluxes of  $\text{H}_2\text{CO}_3$ ,  $J_{\text{H}_2\text{CO}_3}^{\text{C}}$ ;  $\text{HCO}_3^-$ ,  $J_{\text{HCO}_3^-}^{\text{C}}$ ; and  $\text{CO}_3^{2-}$ ,  $J_{\text{CO}_3^{2-}}^{\text{C}}$  in the cathode as well [21],

$$J_{\text{CO}_2}^{\text{evap}} = J_{\text{H}_2\text{CO}_3}^{\text{C}} + J_{\text{HCO}_3^-}^{\text{C}} + J_{\text{CO}_3^{2-}}^{\text{C}}. \quad (10)$$

Since  $\text{HAc}$  and  $\text{Ac}^-$  neither react nor evaporate away from the cathode, the sum of these fluxes equals zero at this interface,

$$J_{\text{HAc}}^{\text{C}} + J_{\text{Ac}^-}^{\text{C}} = 0. \quad (11)$$

Note that Eq. (11) does not imply that the individual fluxes of the ionic species  $\text{HAc}$  and  $\text{Ac}^-$  are zero in the membrane. Due to the acid-base equilibrations, it is possible that one ion diffuses in one direction through the membrane and gradually converts to the other ion, which diffuses back. The only constraint is that at each position in the membrane the sum of the two fluxes is zero (in steady state).

Finally, the total ionic current is related to the electrical current,  $I$ , according to

$$I = F \sum_i z_i J_i^{\text{C}}. \quad (12)$$

By relating both the hydrogen gas production and the total ionic current to the electrical current via Eqs. (8) and (12), we establish the essential relationships between electron flow and hydrogen flow, without making any statements about which ions in solution “carry” the protons through the membrane, the protons which in the electrode are converted to hydrogen gas. Thus, a reaction such as  $2\text{H}^+ + 2\text{e}^- \longleftrightarrow \text{H}_2(\text{g})$  is not explicitly used. Instead, all amphoteric ions in solution may participate in carrying the protons to the electrode and the gas/liquid interface, where they are converted to hydrogen gas.

### C. Evaporation of $\text{NH}_3$

In the cathode, three-phase contact between the electron-conductive matrix, the gas phase, and the liquid phase is established. We assume that the ionic transport in the electrolyte-filled porous cathode is much faster than in the membrane. Thus, we do not need to model ionic transport from the membrane through the cathode to the gas/liquid interface. We relate the partial gas pressure of the gases  $\text{CO}_2$  and  $\text{NH}_3$  to the evaporative fluxes as described by Eqs. (9) and (10) according to

$$p_i = p_{\text{tot}} \frac{J_i^{\text{evap}}}{\sum_n J_n^{\text{evap}} + J_{\text{G}}^{\text{inert}}}, \quad (13)$$

where  $p_i$  is the partial pressure of gas  $i$ ,  $p_{\text{tot}}$  the total pressure in the cathode chamber,  $J_{\text{G}}^{\text{inert}}$  an inert-gas flow along the cathode, and where  $n$  runs over other gases that evaporate from the cathode ( $\text{NH}_3$ ,  $\text{H}_2$ , and  $\text{CO}_2$ ). The inert-gas flow rate  $J_{\text{G}}^{\text{inert}}$  has dimension  $\text{mol m}^{-2} \text{s}^{-1}$  by dividing its molar flow rate ( $\text{mol/s}$ ) by the membrane area ( $\text{m}^2$ ). The relation between the concentration of the soluble gases, in this case  $\text{CO}_2$  and  $\text{NH}_3$ , in the cathode, and the partial pressure of these gases, is given by Henry’s law,

$$c_{C,i} = K_{H,i} p_i, \quad (14)$$

with  $K_{H,i}$  Henry’s coefficient and  $c_{C,i}$  the ion concentration in the electrolyte within the cathode. For  $\text{CO}_2$ , here we assume that the equilibration between unhydrated and hydrated  $\text{CO}_2$  in water is infinitely fast, which is actually considered to be a slow equilibration [39]. The concentration of the ions in the cathode follows from the concentration just in the membrane according to the Donnan equilibrium, as given by Eq. (7), where, for this boundary,  $c_{\text{an},i}$  is replaced by  $c_{C,i}$ . Furthermore, we use the charge neutrality equation, Eq. (2), for the electrolyte within the cathode. Note that we have not considered the evaporation

of water in our model, which would lead to about 3 vol% water molecules in the gas phase at ambient conditions.

### III. RESULTS AND DISCUSSION

#### A. Parameter settings

The model is used to simulate the evaporation, and thus the recovery, of ammonia gas from urine in a U-MEC, as well as the evaporation of  $\text{CO}_2$  and the electrochemical production of hydrogen gas. The calculations are performed using the current as an independent variable. To investigate the influence of the membrane type, we calculate the ammonia evaporation for three different configurations of a U-MEC. The first configuration includes a 4M cation exchange membrane (CEM), which represents the commercially available Nafion N117 membrane used in the U-MFC setup of Kuntke *et al.* [14]. The second configuration includes what we call a zero-charge membrane (ZCM), i.e., an uncharged porous layer ( $\omega X = 0$ ), which neither enhances nor retards the transport of cations or anions. Thirdly, we calculate the ammonia evaporation for a configuration including a 4M anion exchange membrane (AEM). The parameters used for the simulations are listed in Table I.

#### B. Hydrogen production and ammonia recovery as a function of the current density

Obviously, the hydrogen gas production is proportional to the current density, as given by Eq. (11); see Fig. 3. Regarding the evaporation rate of  $\text{NH}_3$ , Fig. 3 shows a linear increase of the ammonia evaporation flux,  $J_{\text{NH}_3}^{\text{evap}}$ , as a function of the current, which is the same for a configuration with a 4M CEM membrane as for the case of a ZCM. As for every electron transported (and for every half an  $\text{H}_2$  molecule produced), a proton, which is most likely shuttled by ammonium ions, is expected to be transported from the anode chamber to the cathode, one would expect a higher ammonia recovery than calculated, more closely to the upper dashed line denoted “Ideal ammonia recovery” in Fig. 3. To understand why the real ammonia recovery is lower than the ideal ammonia recovery, the fluxes of both ammonia and ammonium at the

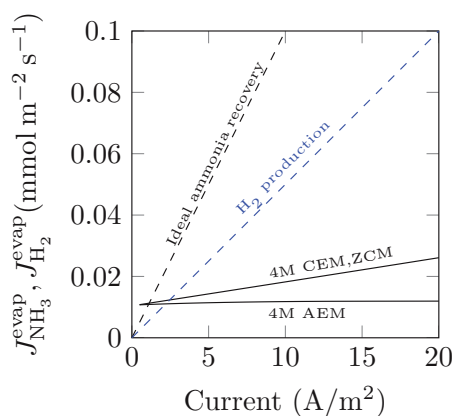


FIG. 3. (Color online) Ammonia evaporation rate,  $J_{\text{NH}_3}^{\text{evap}}$  (solid lines), and hydrogen production rate,  $J_{\text{H}_2}^{\text{evap}}$ , as function of current for a 4M CEM, a ZCM, and a 4M AEM configuration.

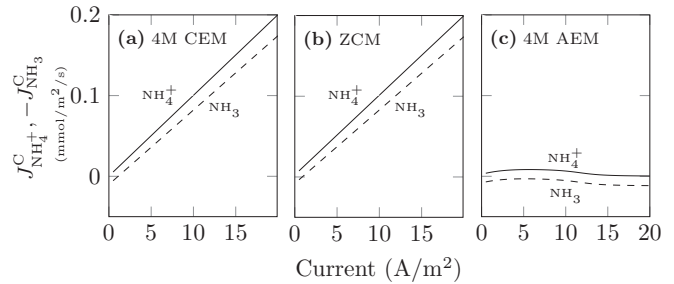


FIG. 4. Fluxes of  $\text{NH}_4^+$ ,  $J_{\text{NH}_4^+}^{\text{C}}$  (solid lines), and  $\text{NH}_3$ ,  $J_{\text{NH}_3}^{\text{C}}$  (dashed lines), at the membrane/cathode interface, as a function of current. The difference between these two fluxes is the evaporation rate of gaseous ammonia; see Fig. 3.

membrane/cathode interface (i.e., at the right-hand side of the membrane) are plotted in Fig. 4. According to Fig. 4(a) (configuration with a 4M CEM), the ammonium flux is almost equal to the “Ideal ammonia recovery.” However, 87% of the ammonia ( $\text{NH}_3$ ) produced in the cathode does not evaporate but, instead, diffuses back to the anode chamber through the membrane, and only the difference between the ammonium flux to the cathode and the ammonia flux from the cathode equals the net ammonia evaporation flux,  $J_{\text{NH}_3}^{\text{evap}}$ , as given in Fig. 4. For a ZCM, the same effect is calculated; see Fig. 3(b). So, for both the 4M CEM and the ZCM, we calculate that only 13% of the electrons transported from the anode to the cathode result in the recovery of an ammonia molecule. These findings, of the low ammonia evaporation flux compared to the current, are broadly in line with the results of experimental U-MFC and U-MEC research as reported in Refs. [14,15], where the authors report that ammonia recovery is about 30% of the maximum value, which is the current divided by Faraday’s number,  $F$ .

Furthermore, Fig. 3 shows that when a 4M AEM is incorporated in the cell, the evaporation flux of  $\text{NH}_3$  is

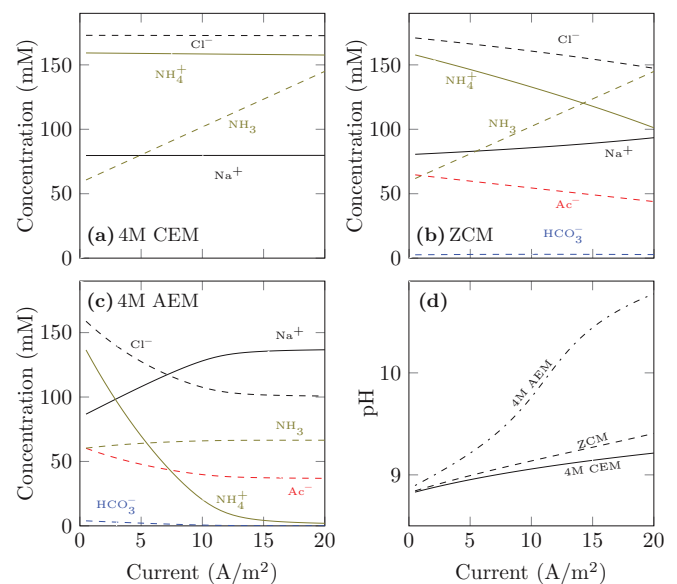


FIG. 5. (Color online) Ion concentrations and pH in the cathode as a function of current for a 4M CEM, a ZCM, and a 4M AEM. Species that are not plotted have negligible concentrations.

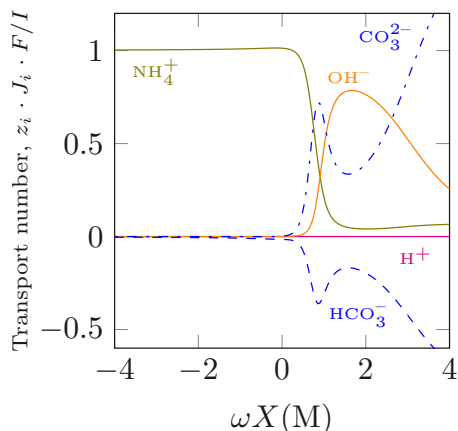


FIG. 6. (Color online) Ion transport numbers, that is, the flux of an ionic species multiplied by its valence and divided by the current, as a function of the membrane charge density  $\omega X$  ( $I = 10 \text{ A/m}^2$ ).

lower than in a 4M CEM or a ZCM cell. The lower  $\text{NH}_3$  evaporation in a 4M AEM configuration is caused by the positive background charge of the membrane, which opposes cations to be transported to the cathode. This effect can also be observed in Fig. 4(c): the 4M AEM is hardly permeable for  $\text{NH}_4^+$ , and consequently, independent of current, the flux of  $\text{NH}_4^+$  to the cathode is much smaller than values shown in Figs. 4(a) and 4(b). But why is the ammonia evaporation flux not close to 0 if  $\text{NH}_4^+$  can barely be transported through the membrane? This is due to the fact that the membrane is also permeable for uncharged species such as  $\text{NH}_3$ . As Fig. 4(c) shows, the backward flux of  $\text{NH}_3$  is negative, which means that  $\text{NH}_3$  is actually transported *toward* the cathode when a 4M AEM membrane is employed.

For illustrative purposes, we present in Fig. 5 the ion concentrations in the cathode as a function of the current density for all three membranes. Figure 5 shows how all ion concentrations are dependent on current and membrane charge. A marked effect is that the pH increases when the membrane charge becomes positive (AEM). Because the pH is of importance for the ammonium-ammonia equilibration, it would be interesting to measure the pH for cell configurations with a 4M CEM, a ZCM, and a 4M AEM, and to compare experimental results with calculations.

### C. Effect of membrane properties on the ammonia recovery

In the preceding section we used our model to show the effect of different types of membranes on the evaporation rate of  $\text{NH}_3$ . We observed that the evaporation of  $\text{NH}_3$  as a function of current was almost equal in the 4M CEM and ZCM configurations, while employing a 4M AEM considerably reduced the evaporation rate of ammonia. Because of this unexpected trend, we will discuss the effect of the membrane charge in more detail. Therefore, we studied the transport of the ionic species through the membrane, the evaporation rate of  $\text{NH}_3$ , and the concentration of  $\text{NH}_4^+$  and pH in the cathode, all as a function of the membrane charge in the range from  $-4$  to  $+4$  M. Results are presented in Figs. 6 and 7.

First of all, we discuss the effect of the membrane charge on the transport through the membrane. Because we are interested

in the contribution of each ionic species to the transport of charge, we plot the transport number, i.e., the flux of an ionic species times its charge number divided by the current, as a function of the membrane charge density  $\omega X$  (Fig. 6) [41]. Note that we evaluate the ionic fluxes at the membrane/cathode interface.

Figure 6 illustrates that a membrane with a negative background charge (CEM) is mainly transporting the charge in the form of  $\text{NH}_4^+$ . Although the background charge is negative and therefore a high transport number of  $\text{H}^+$  is expected, Fig. 6 shows that for  $\text{H}^+$  the transport number is very low (always below  $10^{-6}$ ). This can be explained by the high pH, and thus a low  $\text{H}^+$  concentration, which results in a low  $\text{H}^+$  flux between the anode chamber and the cathode.

When the membrane charge increases from  $-4$  to  $0$  M, the transport number of the ions does not change significantly. It is only when the membrane charge increases to beyond  $0$  M that we see a sudden drop of the transport number for  $\text{NH}_4^+$ , while we observe a sudden increase in the transport number of  $\text{OH}^-$ . Now, the current is no longer carried by  $\text{NH}_4^+$  moving from the anode chamber to the cathode, but more and more by  $\text{OH}^-$  moving in the reverse direction.

Figure 6 also shows that when the membrane charge is increased to beyond  $0.3$  M, the transport number for  $\text{CO}_3^{2-}$  increases and the transport number for  $\text{HCO}_3^-$  becomes negative, which means that  $\text{CO}_3^{2-}$  ions are transported from the anode chamber to the cathode, where they bind a proton, and subsequently  $\text{HCO}_3^-$  diffuses to the anode chamber.

### D. Enhanced ammonia recovery with an increased gas flow, or by lowering the pressure

Figure 3 displayed that the ammonia recovery was only 13% of the ideal recovery, an effect due to ammonia backdiffusion from cathode to anode. As we will show next, the extent of ammonia backdiffusion depends on the gas phase pressure and the flow rate of inert gas in the cathode chamber.

Figure 8(a) shows that an increase of the inert-gas flow rate along the cathode,  $J_G^{\text{inert}}$ , results in an increase of the ammonia evaporation for all three membrane configurations. When we compare the ammonia evaporation with the ammonium flux through the membrane, we even observe that the ammonia evaporation can be higher than the membrane flux of ammonium ions. In this case, the uncharged ammonia ion is also transported through the membrane to the gas/liquid interface, not influenced by the electrical current. This extra ammonia evaporation is similar to the stripping of dissolved molecules from a liquid by contacting with a gas phase.

Figure 8(b) shows that decreasing the pressure also results in an increase in ammonia evaporation, independent of the type of membrane applied. Note that lowering the total pressure below the water vapor pressure, 23.2 mbar, would result in the evaporation of water, an effect that was not included in the model.

In summary, using our modeling approach, we demonstrated how we can analyze the factors that determine the rate of ammonia evaporation. We show that ammonia evaporation in a U-MEC is strongly dependent on the gas flow rate along the cathode and on the pressure in the gas diffusion chamber, even

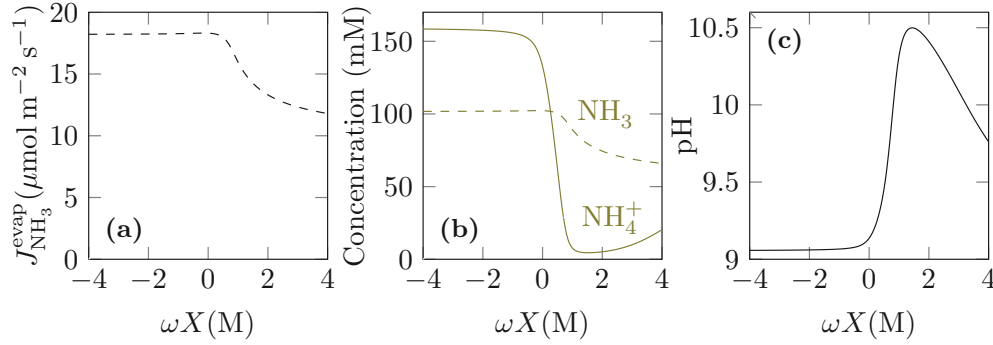


FIG. 7. (Color online) (a) Ammonia evaporation rate, (b) concentrations of  $\text{NH}_4^+$  and  $\text{NH}_3$  in the cathode, and (c) pH in the cathode, all as a function of the membrane charge density  $\omega X$  ( $I = 10 \text{ A/m}^2$ ).

more strongly than the dependence on the electrical current; see Fig. 3.

### E. Discussion on model extensions

In this paper, we described how to model the ionic transport from the anode chamber to the cathode together with simultaneous ion equilibrations. We did not include the mass balances for the anode chamber, but we assumed that the concentrations of the ionic species in the anode chamber were equal to the inflow concentrations. In a more detailed model, this anode chamber can be modeled as an ideally stirred tank

for which mass balances can be formulated again combining individual ion balances to obtain one balance per ion group, just as discussed for the membrane.

The biofilm located on the anode, which was not incorporated in our model, is certainly more complicated to model than the membrane. However, in a first approximation it can be useful to model the biofilm as a film layer, like the membrane, possibly with further reduced ion diffusion coefficients and charge density. At the anode/biofilm interface, details of the bioelectrochemical reaction must be included. Here we will not describe the kinetics of this reaction [42,43], but solely point out how current relates to ionic fluxes (Faradaic stoichiometry) in a numerical scheme using infinitely fast acid-base ion equilibrations. As an example, we consider the important case of the conversion of acetate to bicarbonate, a standard reaction in research in the MFC field.

There is certainly some confusion in the literature about which ions take part in this reaction (e.g., acetic acid or acetate). The elegance of the scheme we present, using at each position in the aqueous volume infinitely fast ion-equilibria (not necessarily infinitely fast Faradaic electrode reactions), is that this question—which ion it is that takes part in the Faradaic electrode reactions—is shown to be of no concern. Instead, the correct description of the boundary condition at the anode is simply that for each ion from the acetate group that reacts away (be it the  $\text{Ac}^-$  ion, or the  $\text{AcH}$  neutral species), eight electrons are injected into the electrode, while two molecules of the carbonate group of ions are formed. Thus, mathematically, the current  $I$  relates to the ion fluxes at the electrode according to

$$\begin{aligned} I &= -8F(J_{\text{AcH}} + J_{\text{Ac}^-}) \\ &= +4F(J_{\text{H}_2\text{CO}_3} + J_{\text{HCO}_3^-} + J_{\text{CO}_3^{2-}}). \end{aligned} \quad (15)$$

For the steady state, the sum of fluxes of each group is invariant with position in the biofilm, and thus the terms  $(J_{\text{AcH}} + J_{\text{Ac}^-})$  and  $(J_{\text{H}_2\text{CO}_3} + J_{\text{HCO}_3^-} + J_{\text{CO}_3^{2-}})$  can be evaluated at any distance from the electrode.

Finally, our model for a MEC could have been used to investigate the ionic transport in an MFC as well, the sole difference being that oxygen is fed together with the inert-gas stream, and must be considered in Eq. (13). In this case, for an MFC, Eq. (8) is replaced by a relation between the consumption of oxygen,  $\text{O}_2(\text{g})$ , and the current (four times the oxygen gas consumption). No other changes are required.

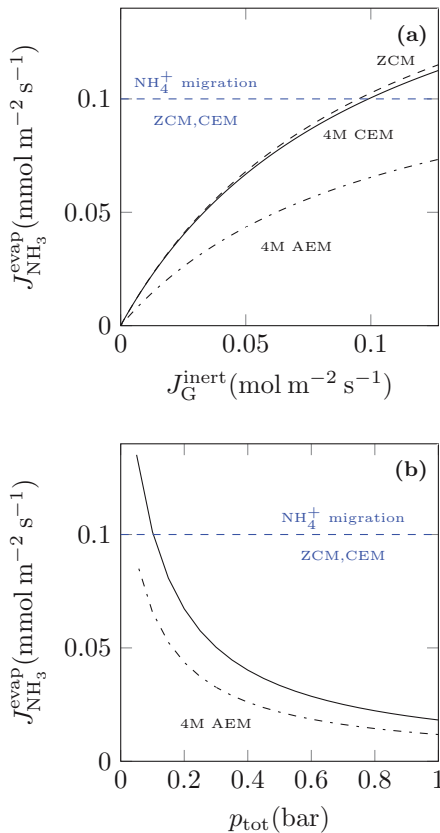


FIG. 8. (Color online) Ammonia evaporation flux on the cathode as a function of (a) the inert gas flow rate, and (b) the pressure in the cathode chamber ( $I = 10 \text{ A/m}^2$ ) for the three different membrane types: 4M CEM, ZCM, and 4M AEM.

#### IV. CONCLUSIONS

In this work we have set up a one-dimensional model for the cathode side of a bioelectrochemical system (BES), a model that describes the simultaneous multi-ionic transport through an ion-exchange membrane placed in the system and the ion acid-base reactions, such as between ammonia and the ammonium ion. To describe these reactions, the local attainment of chemical equilibrium is always assumed, which allows us to neglect details of the rate equations and to replace kinetic rate equations by chemical equilibrium. We include the appropriate boundary conditions to relate the transport through the membrane to the electrical current and to the evaporation of gases in the cathode. In the model, we assume that the formation of hydrogen gas is the only occurring Faradaic reaction in the cathode. However, we do not have to assume which of the ions shuttles the protons through the membrane, or whether the protons or hydroxyl ions directly transfer to the electrode to play a role in the hydrogen gas production. Instead, the transport model self-consistently calculates the contribution of each ion to the current and to the hydrogen gas formation. The model robustly calculates ion transport rates in the steady state in a urine microbial electrolysis cell (U-MEC), a specific BES that recovers ammonia, as well as energy (in the form of H<sub>2</sub>) from urine.

We showed that the ammonia evaporation rate in a cell with a zero charge membrane (ZCM), which is an uncharged

layer that neither enhances nor hinders the transport of charged entities, is as high as the evaporation rate in a configuration with a 4M cation exchange membrane (CEM). This result is clearly counterintuitive. Instead, it was hypothesized that a 4M CEM U-MEC would show a higher ammonia evaporation flux than the ZCM configuration.

The calculations show a low ammonia recovery: a maximum of 13% of the transported electrons from the anode to the cathode is used for the evaporation of ammonia molecules (ZCM/4M CEM configuration), while very close to 100% of the electrons is used for the transport of ammonium through the membrane. The most important reason for this observation is the diffusion of the ammonia molecule from the cathode back to the anode chamber. We find that increasing the inert gas flow along the cathode increases the evaporation rate of ammonia, and the same effect is found when the gas pressure in the cathode gas chamber is decreased.

#### ACKNOWLEDGMENTS

Part of this work was performed in the cooperation framework of Wetsus, centre of excellence for sustainable water technology ([www.wetsus.nl](http://www.wetsus.nl)). Wetsus is cofunded by the Dutch Ministry of Economic Affairs and Ministry of Infrastructure and Environment, the European Union Regional Development Fund, the Province of Fryslân, and the Northern Netherlands Provinces.

- 
- [1] Z. Du, H. Li, and T. Gu, *Biotechnol. Adv.* **25**, 464 (2007).
- [2] P. Clauwaert, P. Aelterman, T. H. Pham, L. De Schampelaire, M. Carballa, K. Rabaey, and W. Verstraete, *Appl. Microbiol. Biotechnol.* **79**, 901 (2008).
- [3] K. Rabaey and W. Verstraete, *Trends Biotechnol.* **23**, 291 (2005).
- [4] L. M. Tender, C. E. Reimers, H. A. Stecher, D. E. Holmes, D. R. Bond, D. A. Lowy, K. Pilobello, S. J. Fertig, and D. R. Lovley, *Nat. Biotechnol.* **20**, 821 (2002).
- [5] H. V. M. Hamelers, A. Ter Heijne, T. H. J. A. Sleutels, A. W. Jeremiasse, D. P. Strik, and C. J. N. Buisman, *Appl. Microbiol. Biotechnol.* **85**, 1673 (2010).
- [6] A. Ter Heijne, H. V. M. Hamelers, V. De Wilde, R. A. Rozendal, and C. J. N. Buisman, *Env. Sci. Technol.* **40**, 5200 (2006).
- [7] D. Call and B. E. Logan, *Env. Sci. Technol.* **42**, 3401 (2008).
- [8] B. E. Logan, D. Call, S. Cheng, H. V. M. Hamelers, T. Sleutels, A. W. Jeremiasse, and R. A. Rozendal, *Env. Sci. Technol.* **42**, 8630 (2008).
- [9] T. H. J. A. Sleutels, H. V. M. Hamelers, R. A. Rozendal, and C. J. N. Buisman, *Int. J. Hydrogen Energy* **34**, 3612 (2009).
- [10] M.-F. Manuel, V. Neburchilov, H. Wang, S. R. Guiot, and B. Tartakovsky, *J. Power Sources* **195**, 5514 (2010).
- [11] H.-S. Lee, C. I. Torres, P. Parameswaran, and B. E. Rittmann, *Env. Sci. Technol.* **43**, 7971 (2009).
- [12] K. M. Udert, T. A. Larsen, and W. Gujer, *Water Sci. Technol.* **54**, 413 (2006).
- [13] T. A. Larsen and W. Gujer, *Water Sci. Technol.* **34**, 87 (1996).
- [14] P. Kuntke, K. M. Smiech, H. Bruning, G. Zeeman, M. Saakes, T. Sleutels, H. V. M. Hamelers, and C. J. N. Buisman, *Water Res.* **46**, 2627 (2012).
- [15] P. Kuntke, T. Sleutels, M. Saakes, and C. Buisman, *Int. J. Hydrogen Energy* **39**, 4771 (2014).
- [16] R. Cord-Ruwisch, Y. Law, and K. Y. Cheng, *Bioresource Technol.* **102**, 9691 (2011).
- [17] M. Maurer, P. Schwegler, and T. A. Larsen, *Water Sci. Technol.* **48**, 37 (2003).
- [18] P. Kuntke, M. Geleji, H. Bruning, G. Zeeman, H. V. M. Hamelers, and C. J. N. Buisman, *Bioresource Technol.* **102**, 4376 (2011).
- [19] A. W. Jeremiasse, H. V. M. Hamelers, J. M. Kleijn, and C. J. N. Buisman, *Env. Sci. Technol.* **43**, 6882 (2009).
- [20] A. Missner, P. Kügler, S. M. Saparov, K. Sommer, J. C. Mathai, M. L. Zeidel, and P. Pohl, *J. Biol. Chem.* **283**, 25340 (2008).
- [21] R. J. Helder, *Plant Cell Environ.* **8**, 399 (1985).
- [22] A. K. Marcus, C. I. Torres, and B. E. Rittmann, *Bioresource Technol.* **102**, 253 (2011).
- [23] A. R. C. Duarte, C. Martins, P. Coimbra, M. H. M. Gil, H. C. de Sousa, and C. M. M. Duarte, *J. Supercrit. Fluids* **38**, 392 (2006).
- [24] D. N. Espinoza and J. C. Santamarina, *Water Resources Res.* **46**, W07537 (2010).
- [25] S. Ebrahimi, C. Picioreanu, R. Kleerebezem, J. J. Heijnen, and M. C. M. Van Loosdrecht, *Chem. Eng. Sci.* **58**, 3589 (2003).
- [26] G. Astarita and D. W. Savage, *Chem. Eng. Sci.* **35**, 1755 (1980).
- [27] P. Gerard, G. Segantini, and J. Vanderschuren, *Chem. Eng. Sci.* **51**, 3349 (1996).
- [28] D. R. Olander, *AIChE J.* **6**, 233 (1960).
- [29] P. Turjanski, N. Olaiz, R. Abou-Adal, C. Suarez, M. Risk, and G. Marshall, *Electrochim. Acta* **54**, 6199 (2009).

- [30] C. Picioreanu, M. C. M. van Loosdrecht, T. P. Curtis, and K. Scott, *Bioelectrochemistry* **78**, 8 (2010).
- [31] Y.-L. Hwang and F. G. Helfferich, *Reactive polymers* **5**, 237 (1987).
- [32] M. B. Andersen, M. van Soestbergen, A. Mani, H. Bruus, P. M. Biesheuvel, and M. Z. Bazant, *Phys. Rev. Lett.* **109**, 108301 (2012).
- [33] J. M. Paz-Garcia, O. Schaetzle, P. M. Biesheuvel, and H. V. M. Hamelers, *J. Coll. Interf. Sci.* **418**, 200 (2014).
- [34] M. Bercovici, S. K. Lele, and J. G. Santiago, *J. Chromatogr. A* **1216**, 1008 (2009).
- [35] O. A. Palusinski, M. Bier, and D. A. Saville, *Biophys. Chem.* **14**, 389 (1981).
- [36] D. A. Saville and O. A. Palusinski, *AIChE J.* **32**, 207 (1986).
- [37] A. H. Galama, J. W. Post, M. A. Cohen Stuart, and P. M. Biesheuvel, *J. Membrane Sci.* **442**, 131 (2013).
- [38] R. N. Bennett, P. D. Ritchie, D. Roxburgh, and J. Thomson, *Trans. Faraday Soc.* **49**, 925 (1953).
- [39] R. J. Helder, *Plant Cell Environ.* **11**, 211 (1988).
- [40] W. Stumm and J. J. Morgan, *Aquatic Chemistry—Chemical Equilibria and Rates in Natural Waters* (Wiley, New York, 1995).
- [41] A. Persat, M. E. Suss, and J. G. Santiago, *Lab Chip* **9**, 2454 (2009).
- [42] H. V. M. Hamelers, A. Ter Heijne, N. Stein, R. A. Rozendal, and C. J. N. Buisman, *Bioresource Technol.* **102**, 381 (2011).
- [43] R. Rousseau, M.-L. Délia, and A. Bergel, *Energy Environ. Sci.* **7**, 1079 (2014).